J of Nuclear Medicine Technology, first published online January 4, 2023 as doi:10.2967/jnmt.122.264834

Confirmation of Intracranial Neuroendocrine Metastasis Utilizing ^{68}Ga-DOTATATE PET/CT

Authors: Rahim Ismail, MD, Mark Manganaro DO, James Bai, MD

Department of Imaging Science, University of Rochester Medical Center, Rochester, NY

Nothing to disclose.

*Corresponding Author:

Mark Manganaro, DO

Mark_manganaro@urmc.rochester.edu

601 Elmwood Ave Rochester, NY 14642

Abstract

Neuroendocrine tumors (NETs) are rare neoplasms with an exceedingly low incidence of intracranial metastasis. We present a 79-year-old female with a biopsy-proven pulmonary neuroendocrine tumor who presented with an intracranial mass in the posterior fossa that was DOTATATE avid on a ^{68}Ga-DOTATATE PET/CT, facilitating the rare diagnosis of intracranial NET metastasis. The case highlights the utility of advanced imaging techniques in differentiating intracranial NET metastasis from other etiologies.

Background

Neuroendocrine tumors (NETs) typically present in an indolent clinical course, with an incidence of 6.98 per 100,000 (1). These lesions primarily, but not exclusively, originate from the gastrointestinal and bronchopulmonary system (2). Intracranial metastases of NETs are rare, with an estimated incidence of 1.5%-5% (2, 3). The sites of spread within the brain intracranial metastasis are relatively uncharacteristic, with reported intracranial metastatic disease in the parenchyma, pineal gland, posterior fossa, dura, and even within a skull base an existing meningioma (4,5).

Prognosis can vary depending on the NET stage and site of origin. Registry data on 10-year specific survival rates of 6792 patients with small intestine NETs, found prognosis of locally advanced disease ranging from 77-95%, nodal disease from 68-77% and distant metastatic disease at 42%. The median survival time after diagnosis of brain metastasis was found to be 10.0 months; however, this increased to 3.2 years in patients who underwent resection and whole brain radiation therapy (3). Therefore, accurate diagnosis of intracranial metastases of NETs plays an important role in providing reliable prognoses and clinical management.

A rare clinical scenario is a patient with multiple potential primary oncologic processes, making accurate diagnoses more critical for guiding clinical management. We present the case of a 79-year-old female with biopsy-proven pulmonary NET and additional incidental renal and thyroid lesions who presented with a symptomatic posterior fossa mass with avidity on ^{68}Ga-DOTATATE PET/CT, leading to a diagnosis of intracranial NET metastasis.

Case Presentation

The patient is a 79-year-old female who presented for progressive gait instability over 5 months. MRI demonstrated a 2.9 cm avidly enhancing intracranial mass in the cerebellum containing intralesional hemorrhage (Figure 1). CT Chest, Abdomen, and Pelvis showed a dominant 4.1 cm left upper lobe lung mass (Figure 2C) and several lung nodules throughout the bilateral lungs. CT-guided lung biopsy proved "epithelial neoplasm with neuroendocrine differentiation, favor carcinoid tumor."

[18F]-fluoro-2-deoxy-d-glucose positron emission tomography (FDG-PET) CT demonstrated hypermetabolism of the left lung mass (Figure 3A). The intracranial lesion has similar FDG uptake compared to the surrounding hypermetabolic brain (Figure 3B). Additional metastatic workup revealed two additional lesions: a small 1 cm enhancing right renal lesion and a heterogeneous hypodense left thyroid nodule, both of which have known propensities for intracranial hemorrhagic metastases. ^{68}Ga-DOTATATE PET/CT demonstrated corresponding DOTATATE uptake within the focal lesion in the right cerebellum (Figure 2A) and left lung mass, confirming somatostatin receptor expressions in these lesions.

In this case, intracranial metastases from the thyroid gland and the kidney are essentially excluded as feasible diagnoses given the ^{68}Ga-DOTATATE uptake. Other intracranial lesions that exhibit ^{68}Ga-DOTATATE uptakes include meningiomas and hemangioblastomas. However, of intra-tumoral hemorrhage in meningioma is rare and hemangioblastomas demonstrate mural enhancing nodules with cystic components on the structural brain MRI exam. Given the presumed recent onset, the ^{68}Ga-DOTATATE avidity, and hemorrhage, the lesion in this clinical context would likely be a neuroendocrine metastasis.

The patient received four days of Stereotactic radiotherapy (SRT) using volumetric modulated arc therapy (VMAT) for a total of 3000 cGY in 5 fractions. On three months post-treatment follow-up MRI exam, the lesion decreased in size and enhancement. The pulmonary lesions were monitored due to lack of associated symptoms.

Discussion

NET's are a rare and diverse group of neoplasms that are generally follow an indolent course with a high propensity to metastasize. Intracranial NET metastases are extremely rare, with variable imaging characteristics and distributions on imaging when described in the literature. Functional data from ^{68}Ga-DOTATATE PET/CT provides additional valuable information for lesion characterization, increasing diagnostic accuracy for NET intracranial metastases. 68Ga radiopharmaceuticals have been utilized for the diagnosis and staging of NETs for multiple reasons. The NET's somatostatin receptor type 2 expression allows for somatostatin analog radiopharmaceuticals to be utilized for the identification of tumors. The gold standard for detection and staging of most NETs is (111) Indium-DTPA-octreotide with a sensitivity of between 50% and 95%, depending on the subtype of NET (6). However, 68Ga, when linked to a DOTA peptide, demonstrates an increased affinity for this somatostatin receptor subtype 2, with the highest affinity being seen in ^{68}Ga-DOTATATE (7). Ga-68 DOTATATE has been shown to be useful in identifying the primary and metastatic NETs which express the somatostatin receptor (6). Recent European guidelines regarding imaging in search of a primary NET include cross-sectional imaging with CT and/or MRI, followed by ^{68}Ga-DOTATATE PET in combination with native or triple-phase enhanced CT (813).

Although ^{68}Ga-DOTATATE PET/CT helps to distinguish intracranial metastases from NETs versus other primary neoplasms, other intracranial lesions express somatostatin receptors, particularly meningiomas and hemangioblastomas, can also demonstrate DOTATATE uptake. *Oh et al.* reported a case of a 36-year-old female with Von Hippel Lindau disease in which ^{68}Ga-DOTATATE PET/CT for pancreatic tumor restaging found new cerebellar and spinal hemangioblastomas with DOTATATE uptake (10). In the cases where distinguishing between meningioma/hemangioblastoma and NET are necessary, structural brain MRI and clinical context remain crucial to reaching accurate diagnoses.

Conclusion

Intracranial metastases from NETs are extremely rare and can have uncharacteristic and variable imaging appearances on conventional imaging. Accurate diagnoses of these lesions are important to provide reliable prognoses and to guide appropriate treatment for these patients. The case report demonstrates the utility of ^{68}Ga-DOTATATE PET CT in combination with conventional imaging providing a more robust lesion characterization and accurate diagnosis in this patient with NET intracranial metastasis.

References

1. Dasari A, Shen C, Halperin D, et al. Trends in incidence, prevalence, and survival outcomes in patients with neuroendocrine tumors in the United States. *JAMA Oncol.* 2017;1335-42.

2. Mallory GW, Fang S, Giannini C, Van Gompel JJ, Parney IF. Brain carcinoid metastases: outcomes and prognostic factors. *J Neurosurg.* 2013;118~~(4)~~:889-95.

3. Krug S, Teupe F, Michl P, Gress TM, Rinke A. Brain metastases in patients with neuroendocrine neoplasms: risk factors and outcome. *BMC Cancer.* 2019;19~~(1)~~:362.

4. Bhojwani N, Huang J, Gupta A, Badve C, Cohen ML, Wolansky LJ. Rectal carcinoid tumor metastasis to a skull base meningioma. *Neuroradiol J.* 2016;29~~(1)~~:49-51.

5. Cuoco JA, Kortz MW, McCray E, et al. Case report: metastatic bronchopulmonary carcinoid tumor to the pineal region. *Front Endocrinol (Lausanne)*. 2021;12:623756.

6. Krenning EP, Kwekkeboom DJ, Bakker WH, et al. Somatostatin receptor scintigraphy with [111In-DTPA-D-Phe1]- and [123I-Tyr3]-octreotide: the Rotterdam experience with more than 1000 patients. *Eur J Nucl Med*. 1993;20~~(8)~~:716-31.

7. Hofman MS, Lau WF, Hicks RJ. Somatostatin receptor imaging with 68Ga DOTATATE PET/CT: clinical utility, normal patterns, pearls, and pitfalls in interpretation. *Radiographics*. 2015;35:500-16.

8. Niederle B, Pape UF, Costa F, et al. ENETS Consensus guidelines update for neuroendocrine neoplasms of the jejunum and ileum. *Neuroendocrinology*. 2016;103(2):125-38.

9. Unterrainer M, Ruf V, Ilhan H, et al. 68Ga-DOTATOC PET/CT Differentiates meningioma From dural metastases. *Clin Nucl Med*. 2019; 412-3.

10. Oh JR, Kulkarni H, Carreras C, et. al. Ga-68 somatostatin receptor PET/CT in von Hippel-Lindau Disease. *Nucl Med Mol Imaging.* 2012;46(2):129-33.

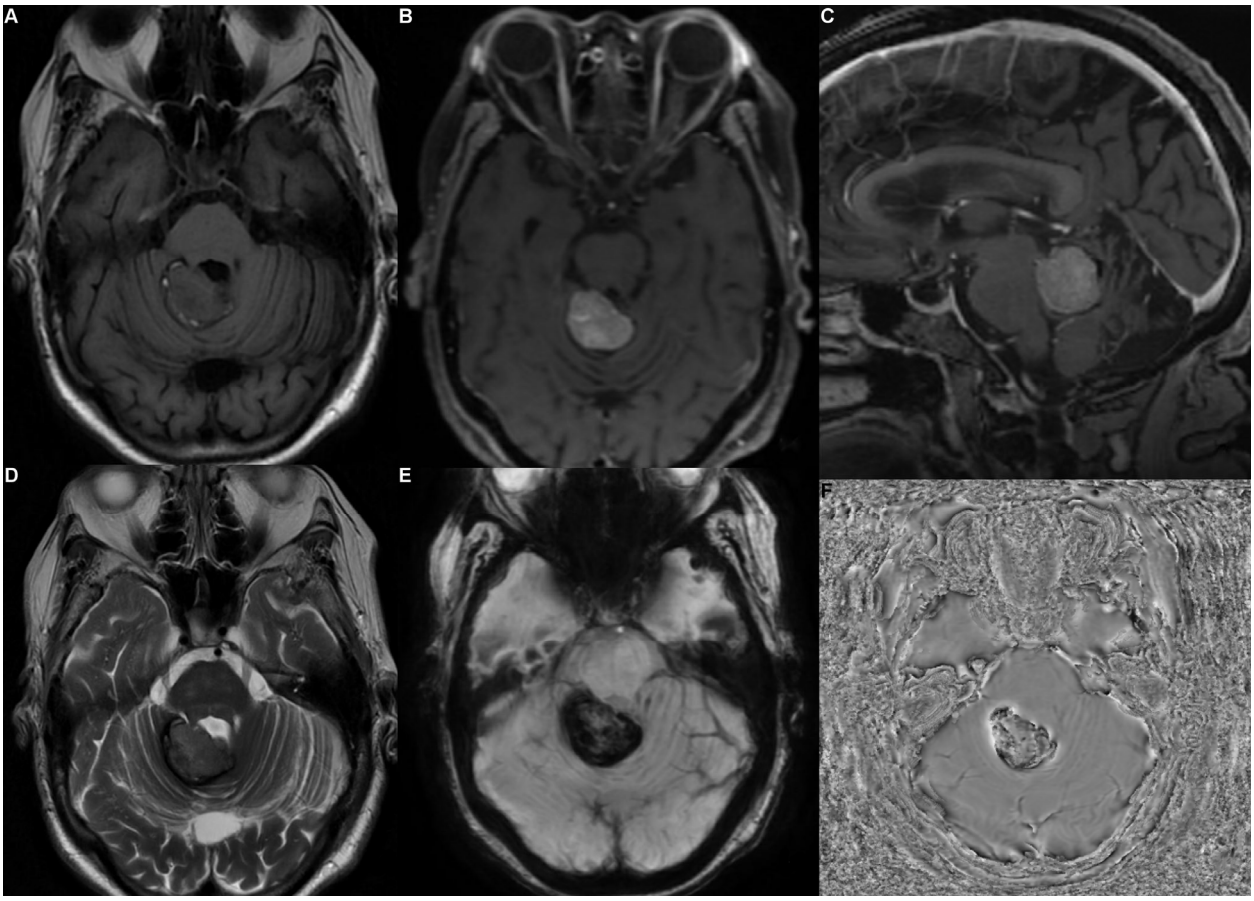

Figure 1: Axial T1 pre-contrast image (A) demonstrates an extra-axial posterior fossa lesion in the right superior cerebellar region, with intermediate T1 signal and intrinsic peripheral T1 hyperintensity. Axial and sagittal T1 post-contrast image (B, C) shows avid enhancement within this lesion. Corresponding axial T2 image (C) demonstrates intermediate signal intensity. Susceptibility weighted image (F) demonstrates susceptibility artifact within the lesion with some corresponding signal loss on the phase image (E), suggesting intralesional hemorrhage.

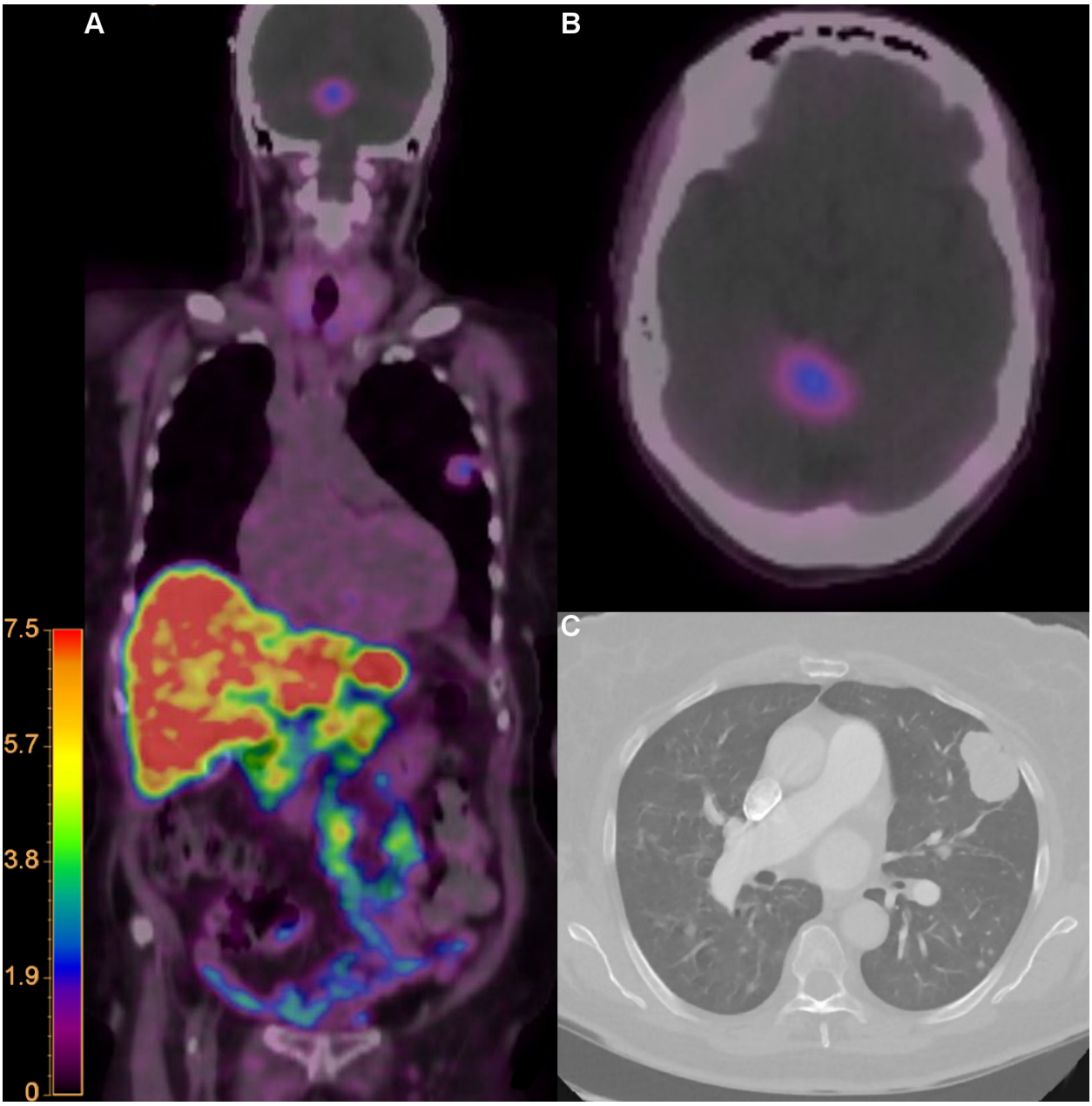

Figure 2: ^{68}Ga-DOTATATE PET/CT demonstrates corresponding DOTATATE uptake of the posterior fossa lesion (A, B) and left lung mass. CT Chest demonstrated a left upper lobe lung mass (C).

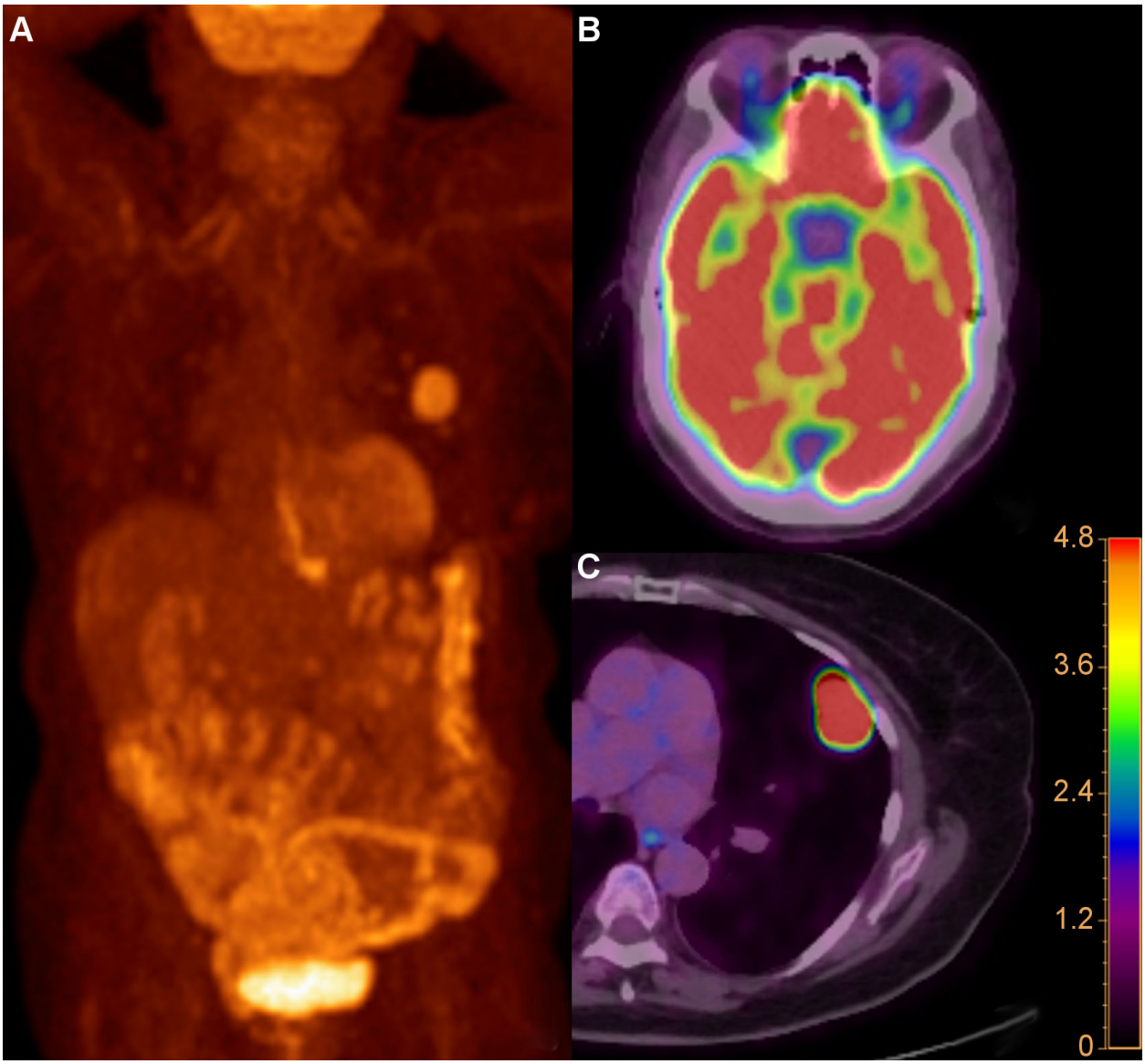

Figure 3: [18F]-fluoro-2-deoxy-d-glucose positron emission tomography (FDG-PET) CT demonstrated hypermetabolism of the left lung mass (Figure 3A and 3C). The FDG uptake of the posterior fossa lesion is similar to the surroundig hypermetabolic brain parenchyma (Figure 3B).